ELSEVIER

Polymer 40 (1999) 7387–7396

polymer

Surface pattern in thin poly(styrene–maleic anhydride) films

Mingtai Wang*, Xiaoguang Zhu, Shixing Wang, Lide Zhang

Institute of Solid State Physics, Chinese Academy of Sciences, Hefei 230031, People's Republic of China

Received 28 July 1998; received in revised form 6 October 1998; accepted 18 December 1998

Abstract

Monodispersed poly(styrene–maleic anhydride) alternating copolymer (SMA) is synthesized through radical polymerization, and characterized by GPC, DSC, FT-IR and ^{1}H NMR spectra. The mole fraction, χ, of styrene in the copolymer is 0.51, determined from integrated ^{1}H NMR spectrum, this value is consistent with the alternating structure. FT-IR spectra show that maleic anhydride moieties on the backbone chains hydrolyze in a THF solution containing water, and HCl can accelerate the hydrolysis process. Atomic force microscopy reveals that well-arrayed and uniform-sized holes formed in thin SMA films on single crystal silicon wafer substrates spin-cast from the THF solutions containing HCl. HCl can also influence hydrogen bonding between the carboxylic acid groups in the THF solution, which is crucial for the formation of holes in the thin films. The volatilization process in the spin-casting is divided into two stages, THF and water volatilization. The formation of holes is interpreted as the trace of water droplets emulsified by the hydrolyzed SMA in the second stage, i.e. water volatilization. Results also indicate that there are both mobile and bound water populations in the solution, and that the bound water is responsible for the hole or valley pattern of these thin films.

Keywords: Atomic force microscopy; Thin polymer film; Poly(styrene–maleic anhydride)

1. Introduction

It has been well-known that both styrene and maleic anhydride copolymerize usually in an alternating way, resulting in a poly(styrene–maleic anhydride) alternating copolymer (SMA) with a highly regular structure [1,2], and the copolymerization often proceeds at a temperature not above 90°C [3]. SMA is a type of important functional copolymer as its anhydride groups on backbone chains can react with other reagents, such as alcohols, amines and water etc., to produce many derivatives. Tredgold and Davis et al. [4,5] used derivatives from SMA to form Langmuir–Blodgett films which exhibit high thermal and mechanical durabilities. Recently, many authors synthesized SMA-inorganic hybrid materials, in which inorganic constituents are chemically bonded to SMA backbone chains via chemical reactions between coupling agents and anhydride moieties [6–8]. In this study, atomic force microscopy (AFM) revealed that thin hydrolyzed SMA films spin-cast on inorganic substrates, such as silicon wafer, quartz and glass slide, and show well-arrayed and uniform-sized holes on the surface. We believe this to be the first observation in describing the well-arrayed and uniform-sized holes in the thin polymer film.

In general, films of thickness < 1000 Å are classified as ultrathin films, and those with thicknesses between 1000 and 10 000 Å are regarded as thin films [9]. Spin-casting widely used in the production of thin films in the semi-conductor industry [10] is often used in the preparation of thin and ultrathin polymer films. This can be achieved by placing a small quantity of polymer solution on a substrate, and rotating the substrate at a particular angular rate for a specified time. Details of spin-casting have been described elsewhere [9,11]. More recently, the studies of the surface pattern of spin-cast thin and ultrathin films are of great interest. However, these studies are confined mainly to the cases of polymer/polymer blends by using a three-composition or ternary system: two polymers in a common solvent [12–16]. For a solvent quench, in which the solvent is removed rapidly from the solution, phase separation of the two polymer components can be observed. The formation of surface patterns is regarded as tracking that underlies phase separation process within these films. AFM results [13,14] showed that the formation of holes in the binary blend thin films is also dependent on substrate and composition. Most studies revealed that surface energy is an important factor in the segregation of blend components, and that the component with the lower surface free energy is generally enriched at the air–polymer interface [13,16].

* Corresponding author. Tel.: + 86-551-5591476; fax: + 86-551-5591434.

E-mail address: wmt@mail.issp.ac.cn (M. Wang)

0032-3861/99/$ - see front matter
PII: S0032-3861(99)00008-7

The well-arrayed and uniform-sized hole pattern in the thin films is expected to be useful for nanoscale fabrication. This pattern may enable the films to act as templates for the formation of well-arrayed nanocrystal domains, as in the case of monodispersed diblock copolymer thin film which offers a well-ordered functionalized domain to accommodate nanocrystals [17] and ceramic templates, such as alumina template [18,19].

This article includes the synthesis of styrene–maleic anhydride alternating copolymer and the description of the surface pattern of the thin SMA films spin-cast from different THF solutions. As these studies are exploratory in understanding the hole pattern in thin hydrolyzed SMA films, we would like to regard our interpretations as being tentative. Our suggestions here are mainly intended to form a hypothetical basis for future experimental design and application of these interesting hole patterns.

2. Experimental

2.1. Synthesis of SMA copolymer

Poly(styrene–maleic anhydride) alternating copolymer (SMA) was synthesized through solution polymerization, as described elsewhere [20]. Purified styrene (18 ml), maleic anhydride (AR) (15 g) and benzene (redistilled before use) (400 ml) were added into a 500 ml round-bottomed flask, and stirred at 60°C to form a clear solution, then a small amount of BPO (recrystallized in methanol before use) was added to the solution and the temperature was evaluated at 80°C–81°C. The solution became turbid about five to ten minutes later, the reaction proceeded smoothly between 80°C and 81°C for an hour, under vigorous stirring. After cooling to room temperature, the resultant was filtered off, washed with benzene (AR). The crude product was dispersed into enough benzene again and refluxed for 24 h, filtered off and washed with benzene. The final product was dried at 80°C under vacuum for 48 h, and weighed about 27 g.

2.2. Preparation of thin film on a substrate

SMA was dissolved in THF (purified and distilled over sodium) overnight, and each THF solution was prepared with an SMA concentration of 1%–2% g ml^{-1}. An appropriate quantity of deionized water was added into the SMA solution and stirred for about 2 and 6 h to obtain two samples without the addition of HCl (labeled as SMA–H_2O–2 and SMA–H_2O–6, respectively). Concentrated HCl (37%) was added to the THF solution of SMA to adjust the pH value in the range of 1–1.5. It was checked by a special indicator paper for pH values in the range between 0.5 and 5 (Third Reagent Plant of Shanghai, China), then water of suitable weight was added in and stirred for 2 h to get samples with the addition of HCl (labeled as SMA–H_2O–HCl). Thin films were spin coated onto pre-cleaned single crystal silicon wafers (RMS roughness = 2.90 Å) at a spin rate of 1400 rpm (8 s), and film thickness was controlled by the concentration of the solution [21]. This procedure results in films of mean thickness of 230–235 nm (evaluated from ellipsometric measurements) when the SMA concentration was 1% g ml^{-1}.

Prior to spin coating, the single crystal silicon wafers were cleaned with "piranha solution", a 30 : 70 mixture of 30% hydrogen peroxide and concentrated sulfuric acid, at 80°C for 1.5 h, followed by extensive rinsing with deionized water, and final rinsing with absolute ethanol, and drying in an oven.

2.3. Instruments and measurements

The number average molecular weight (M_n) of as-synthesized copolymer was 2560, and $M_w/M_n = 1.04$, determined with a WATERS 150-C gel permeation chromatography (GPC) with acetone as solvent and monodispersed polystyrene as standard samples. The mole fraction, χ, of styrene in the copolymer was 0.51, determined from integrated ^1H NMR spectrum which was recorded on a FX-90Q NMR spectrometer with acetone-d_6[i.e. $(CD_3)_2CO$] as solvent and internal standard (2.05 ppm). FT-IR spectra of samples were recorded on a Nicolet Magna-IR™ 750 spectrometer with a maximum resolution of 0.1 cm^{-1}. Samples for IR were prepared in film forms obtained from THF solutions and dried at 80°C under vacuum for 2 d before test. The glass transition temperature, T_g, of as-synthesized SMA was 217°C (measured on a Perkin-Elmer DSC-2C apparatus calibrated with ultrapure indium). The SMA sample (7–8 mg) was heated at 570 K for 3 min to eliminate the thermal history, and quenched to 240 K, then scanned from 240 to 550 K with a heating rate of 20 K min^{-1}. T_g was taken as the midpoint of the heat capacity change.

Thin films not immediately measured by AFM were placed in a desiccator with silica-gel drier until measurements (ca. for 3–4 d). AFM measurements were carried out on a scanning probe microscopy (SPM), and an AutoProbe® CP Proven Performance, Research SPM (Park Scientific Instrument) was used to acquire the topographical AFM images in a non-contact mode (NC-AFM) using silicon cantilevers with a conical tip which has a radius of 100 Å supplied by the manufacturer (Park Scientific Instrument). The tip cantilevers in the dimension of $85 \times 28 \times 1.8$ μm^3 have a force constant of 18 N cm^{-1} and a resonant frequency of 360 kHz. AFM observations were executed in air conditions.

3. Results and discussion

3.1. Characterization of as-synthesized copolymer

Styrene–maleic anhydride copolymers are easily prepared by radial polymerization, which gives a 1 : 1 alternating copolymer (SMA) [1,2,22–24]. The structure of the

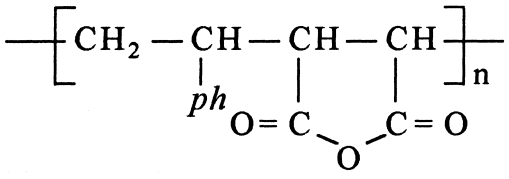

Scheme 1.

alternating copolymer consisting of styrene and maleic anhydride can be shown by Scheme 1 [25–27].

FT-IR and ^{1}H NMR spectra of the as-synthesized copolymer is shown in Fig. 1. The adsorption bands at 1858 and 1778 cm^{-1} in the IR spectrum are characteristic bands of SMA [5,28], assigned to asymmetrical and symmetrical $\nu_{C=O}$ of maleic anhydride moieties [29], respectively. Bands at 1600, 1500 and 1450 cm^{-1} are the $\nu_{C=C}$ of phenyl groups on the backbone [6,29]. The band at 1214 cm^{-1} is attributed to the ν_{C-O-C} of maleic anhydride units, as a five-numbered cyclo-anhydride shows a ν_{C-O-C} band at 1310–1210 cm^{-1} wavenumber [30]. The band at 700 cm^{-1} is the $\delta_{C=C}$ of the phenyl groups [6], which was used as an internal reference to offset differences in the thickness of IR

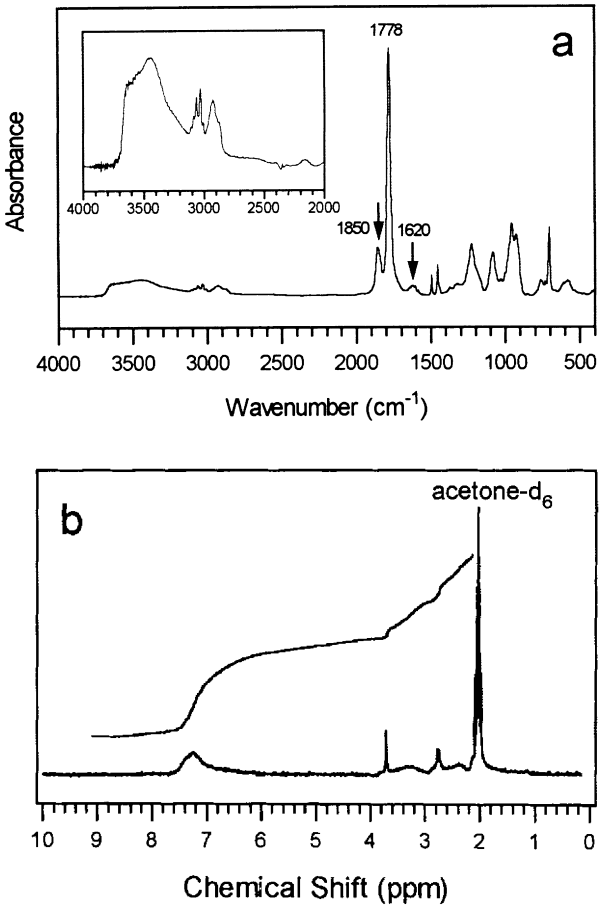

Fig. 1. FT-IR (a) and ^{1}H NMR (b) spectra for poly(styrene–maleic anhydride) alternating copolymer. The IR spectrum in the region of 4000–2000 cm^{-1} is magnified (ca. 8 ×) in absorbance to show the water absorbed in the sample (inset).

samples. The existence of absorbed water from air in this sample can also be indicated by the absorption bands [30] at 1620 cm^{-1}, and the broad band around 3500 cm^{-1} which is shown more clearly by the inset in Fig. 1a.

In the ^{1}H NMR spectrum, the chemical shift of phenyl proton is about 7.30 ppm, and those for –CH– and –CH$_2$– groups on the backbone chains are within 3.80–2.20 ppm. Similar ^{1}H NMR resonance profiles were observed by Dérand et al. [27] in SMA (M_n = 83 000) grafted by poly(ethylene glycol) monomethyl ether when the grafted copolymer was neutralized with LiOH and dissolved in D_2O. However, the assignment of resonance signals in ^{1}H NMR spectrum for the –CH– and CH$_2$– groups on the backbone is hardly available in literature.

It is known [33] that copolymer composition can often be determined from ^{1}H NMR spectra with a probable error within ± 2%, and this method requires that at least one resonance of a functional group in one of the monomer units should be adequately resolved from the rest of the spectrum. Hence, the phenyl group of styrene that appears about 7.30 ppm can be used for the composition analysis. The mole fraction, χ, of styrene in the copolymer was obtained by comparing the integration intensity, I, of phenyl proton with that of the total proton [33,34]. It can be shown that (refer to appendix in the reference section)

$$\chi = \frac{2I_{(\text{phenyl})}}{5I_{(\text{Total})} - 6I_{(\text{phenyl})}}. \quad (1)$$

From the ^{1}H NMR spectrum, the χ of styrene in as-synthesized copolymer was evaluated to be 0.51, this value is consistent with the alternating structure. The ^{13}C NMR spectrum showed that the as-synthesized copolymer has a resonance peak at 35.50 ppm, which indicates that the backbone chains of the copolymer consist of styrene and maleic anhydride monomers in a 1 : 1 alternating way, because the methylene carbons in MSM triad sequences on the copolymer chains of styrene and maleic anhydride show a characteristic resonance at 33–37 ppm [35]. In the investigations of the styrene–maleic anhydride copolymers, ^{13}C NMR spectra are likely to be more revealing than the ^{1}H NMR spectra [26,35], the ^{13}C NMR data of our SMA will appear in another article.

3.2. Surface pattern in thin SMA films

Although scanning tunneling microscopy (STM) was invented first, the current progress of SPM in polymers is largely in the development of AFM [36,37]. AFM has many advantages over traditional transmission electron microscopy (TEM), scanning electron microscopy (SEM), and low voltage high resolution scanning electron microscopy (LVHRSEM), which have been used to study the near-surface or surface morphologies of polymeric materials. Unstained samples can be imaged by AFM under ambient conditions with no special sample preparations.

Fig. 2 shows the typical AFM topologies of thin SMA

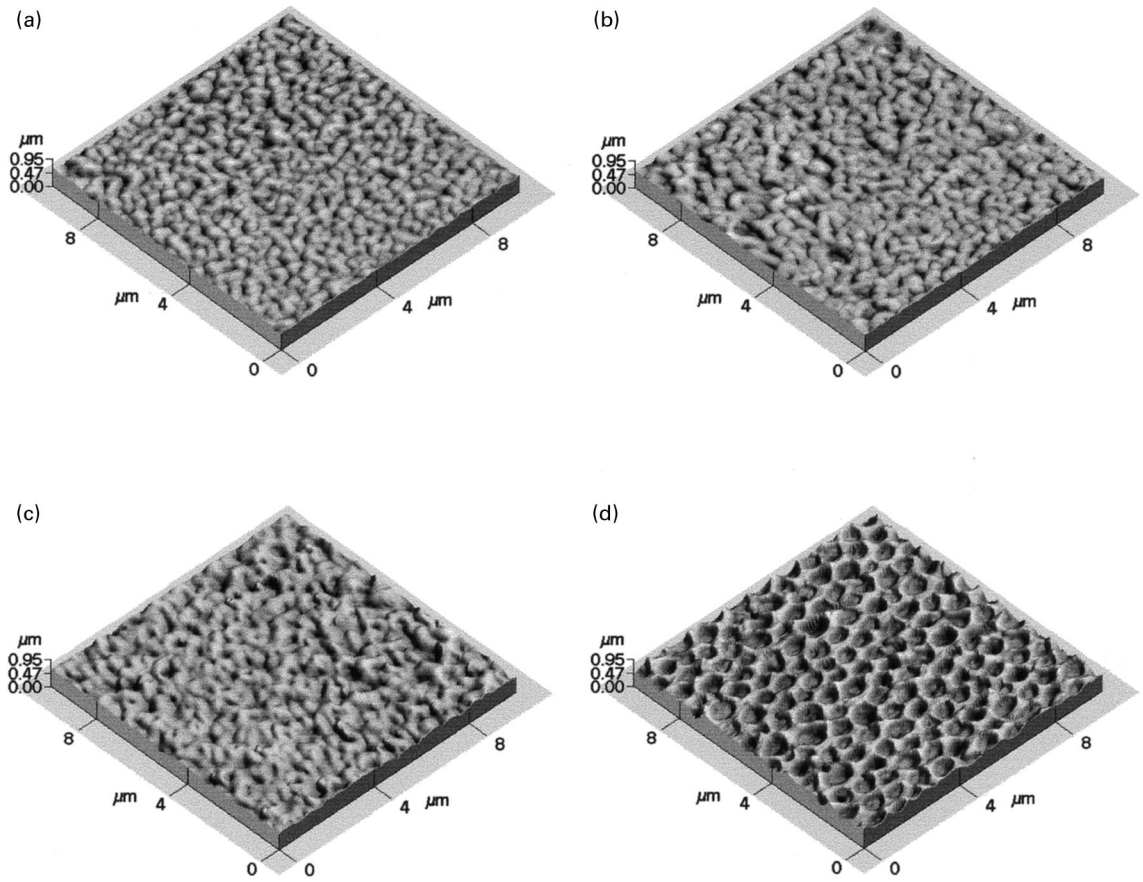

Fig. 2. AFM images of thin films cast from THF solutions with a SMA concentration of 1% g ml^{-1} and weight ratio of H_2O/SMA = 1/3 (a) SMA in THF, RMS = 232 Å; (b) SMA–H_2O–2, RMS = 246 Å; (c) SMA–H_2O–6, RMS = 388 Å; (d) SMA–H_2O–HCl, AFM depth ≈ 0.202 μm.

films spin-cast from different THF solutions. It can be shown that addition of HCl brings out distinct patterns to the surface of thin film. A bicontinuous pattern similar to spinodal decomposition is the characteristic of SMA and SMA–H_2O films without the addition of HCl (Figs. 2a, 2b and 2c) [14,15], but the bicontinuous pattern changes into well-arrayed and uniform-sized holes in SMA–H_2O–HCl samples with the addition of HCl (Fig. 2d). These surface patterns in Fig. 2 were also observed with a SEM, and low magnification views of the specimen surface by SEM revealed the surface patterns to be in a large area with no crack defects (SEM pictures not provided here).

Fig. 3 shows the two-dimensional (2D) image of Fig. 2d and the cross-sectional view along the line in the AFM image, the mean diameter and depth of the holes were obtained from cross-sectional views. The AFM depth of the holes is about 200 nm, and the diameter of the holes is approximately 0.4–0.6 μm. It should be noted that the depth may be a real value, because the diameter of the holes was much larger than that of the conical tip, and the geometry of the conical tip (the sectional triangle of it had a 4 μm height and 20° tip angle) enables the tip to enter the holes.

Fig. 2a shows that the thin SMA film cast from pure THF buckles on the surface, not as a smooth or featureless surface of thin polystyrene film before annealing above T_g [21,38]. It has been generally accepted that the effect of chain end groups on the surface structure and the surface molecular motions can not be ignored, especially in the case of polymers with smaller M_n [16,39–43]. If the magnitude of surface energy ν for the chain end groups, ν_e, is lower than that of the main chain part, ν_m, then the chain end groups are preferentially localized at the surface [44–46], whereas, in the case of $\nu_e > \nu_m$, the chain end groups migrate deeply into the surface interior region [47,48]. As the M_n of SMA in our experiments was small, the end-groups should play an important role in controlling the pattern of thin pure SMA films (Fig. 2a). Hence, it is necessary to determine the end-group structure when we discuss the surface pattern of SMA film.

Let us consider briefly the kinetics in the copolymerization of styrene and maleic anhydride, which is helpful in determining the end-group structure of SMA chains. Great interest has been shown in the kinetics and mechanisms from radical copolymerization that produce highly alternating copolymers. Ebdon et al. [22] gave a detailed review on the alternating copolymerization of styrene and maleic anhydride. Essentially, there are two schools of thoughts concerning the mechanism of alternation in

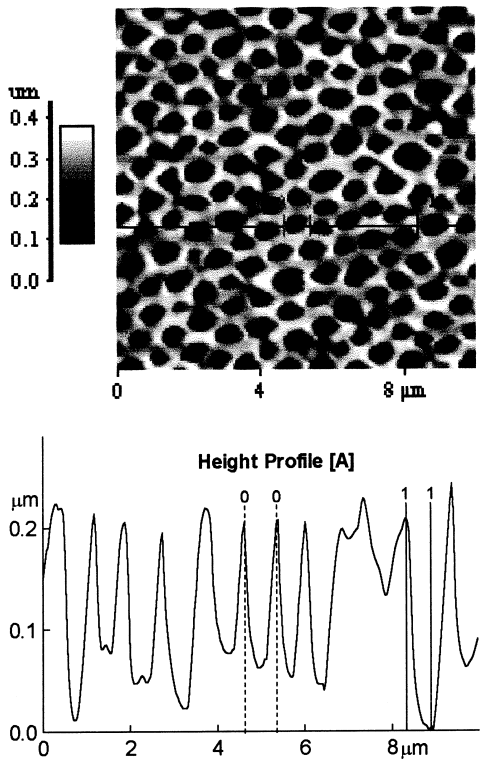

Fig. 3. 2-D AFM image (above) and sectional view (below) along the line in the AFM image for sample SMA–H_2O–HCl of Fig. 2d.

copolymerization of styrene and maleic anhydride. The first maintains that the high degree of alternation is a natural consequence of the reactivities of the monomers and the radicals derived from them, i.e., there is a marked preference for cross-propagation. The second maintains that, to a significant extent, alternation arises from propagation via 1 : 1 monomer–monomer donor–acceptor complexes (i.e. styrene–maleic anhydride complexes) which have a higher reactivity toward the growing radicals than the uncomplexed monomers. The evidence accumulated on the mechanism of this alternating copolymerization suggests that most, if not all, of the alternation arises as a consequence of the relatively rapid cross-propagation reactions [24,49]. The minor anomaly in the copolymerization is most probably a consequence of a penultimate group effect rather than an indication of the involvement of styrene–maleic anhydride complexes. In many solvents, e.g., benzene, dichloroethane and carbon tetrachloride; maximum rates of copolymerization were observed at around the equimolar feed [24,50], and this has been taken as evidence for the involvement of styrene–maleic anhydride complexes. Experiments involving measurements of rates of copolymerization should not be particularly useful because of the large number of parameters needed to describe such rates, as pointed by Ebdon et al. [22].

Fukuda et al. [51] showed that the neglect of small penultimate group effects in the propagation steps can give rise to ϕ value (cross-termination factor), apparently in excess of 1 and the enhanced cross-termination. Deb et al. [23] also showed a detailed kinetic scheme for alternating copolymerization of styrene and maleic anhydride considering both of the above thoughts, in which they showed that over the entire range of monomer feed compositions, the cross-termination of macroradicals is much favored. Sato et al. [52] concluded that styryl and maleic anhydride propagating radicals are present in the polymerizing styrene–maleic anhydride mixtures in ethyl benzene. Based on these studies, the SMA chains should end with two initiator species (i.e. benzoyloxy group in our case).

Though the studies on the kinetics of copolymerization was not detailed, it does not interfere with our discussion, because undoubtedly the end-group is different from the units on the backbone. The buckling on the surface of SMA film is attributed to the difference in the surface free energy, ν, between the end-groups and units on the backbone chains of SMA. The difference between the ν values for these end-groups and units is determined in the further studies on the surface patterns of the thin pure SMA films.

The valley and hole patterns in Figs. 2b and 2d reflect the trace of water domains that are phase-separated from the polymer during the casting process. This can be indicated by the influence of water content on the surface topologies of thin films, as shown in Fig. 4. As the weight ratio of H_2O/SMA is increased from 1/7 to 1/1 in SMA–H_2O–2 systems, the root mean square (RMS) roughness value increased from 237 to 437 Å. At the same time, the valley domains become larger, as shown in Figs. 4a and 4b. As regards the samples of SMA–H_2O–HCl, diameter and depth of holes increased with water content, but the number of holes is reduced in the imaged area ($10 \times 10\ \mu m^2$), refer to Figs. 4c and 4d.

The surface pattern in Fig. 2b should be a combined result of surface energy effect and the trace of water existence. There is no remarkable difference in Fig. 2c, compared with Figs. 2a and 2b, and this case will be discussed in the following section in which the formation of surface pattern in Fig. 2d is described in detail.

3.3. Formation of holes in thin SMA films

3.3.1. The factors determining the formation of holes

Holes on the surface of thin or ultrathin films were also observed in different systems. Reiter [21,38] observed holes in ultrathin polystyrene homopolymer films on silica substrates, and Faldi et al. [53] found holes in the dewetting of one polymer layer from another. The formation of these holes was interpreted in terms of dewetting substrate. Thin and smooth films of these polymers are stable at the temperature well below the glass transition temperature (T_g) or, if crystalline, below the melting point (T_m). However, such polystyrene films may become unstable above T_g. Modulations of the surface induced by thermal fluctuations may increase in amplitude, and eventually hit the substrate. Hence, such films are expected to break up and

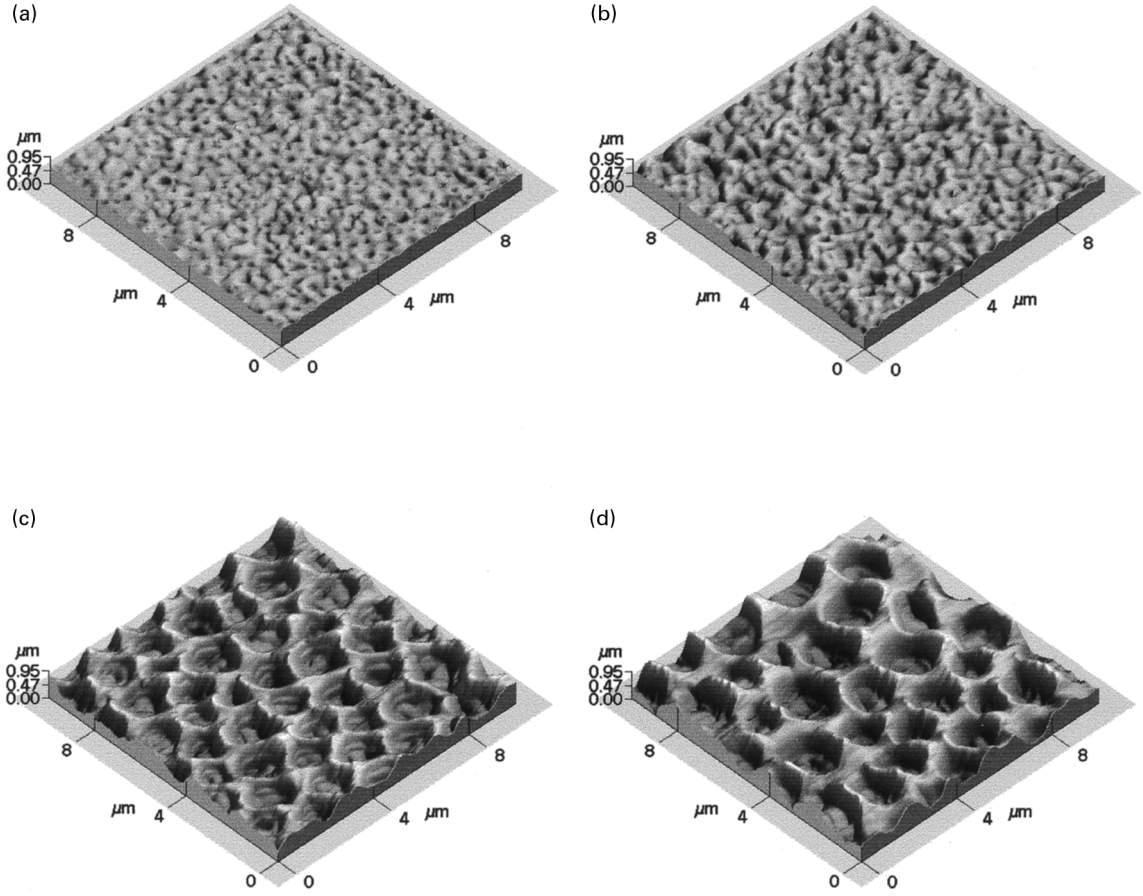

Fig. 4. AFM images of thin films cast from THF solutions with a SMA concentration of 2% g ml^{-1} and different weight ratio of H_2O/SMA: (a) SMA–H_2O–2 with H_2O/SMA = 1/7, RMS = 237 Å; (b) SMA–H_2O–2 with H_2O/SMA = 1/1, RMS = 437 Å; (c) SMA–H_2O–HCl with H_2O/SMA = 1/3, AFM depth ≈ 0.530 μm; (d) SMA–H_2O–HCl with H_2O/SMA = 1/1, AFM depth ≈ 0.670 μm.

minimize the area where the liquid is in contact with the substrate, by a dewetting process [21,38].

Ermi et al. [14] described the phase-separation structures in ultrathin films of deuterated poly(styrene)/poly(vinylmethether)(dPS/PVME) blends via AFM images. Their results show that a bicontinuous spinodal decomposition pattern (similar to Figs. 2a, 2b and 2c) is found for near-critical films, while "mounds" and "holes" are found for PVME-rich and dPS-rich off-critical mixtures, respectively. Buckling of the film boundary was attributed to surface tension variation within the film accompanying phase separation. Mounds and holes in off-critical composition films are attributed to the presence of droplets having higher (dPS) and lower (PVME) surface tensions, respectively.

It is obvious that thermal modulation is an important external factor inducing the formation of holes during dewetting process of homopolymers and phase separation of binary polymer blends. These films were annealed above T_g or T_c (critical temperature of polymer blend) to induce the formation of surface pattern. Our films were not specially treated after casting at any temperature above room temperature, e.g. at 217°C, the T_g of SMA. The surface patterns in our samples were formed during casting, and the as-shown patterns in Fig. 2 can be observed when the films are measured by AFM immediately after cashing. The hole structure, including bicontinuous pattern in our experiments as well, is not a result of temperature modulation, but a direct result of spin-casting. Hence, the surface pattern changes in Fig. 2 may be associated with the intrinsic properties of the copolymer in the films, namely, with the chemical reactions in sample preparations. The samples in Figs. 2b, 2c and 2d were measured by IR spectrometer to determine the chemical reactions taking place during their preparation, and their respective IR spectra are shown in Fig. 5.

Figs. 5b and 5c correspond to the samples in SMA–H_2O–6 and SMA–H_2O–HCl, respectively. Both of them show an adsorption band at 1710 cm^{-1} assigned to the $\nu_{C=O}$ in carboxylic acid groups derived from maleic anhydride moieties [5,6], and bands at 1440–1395 and 1320–1210 cm^{-1} to the δ_{O-H} and ν_{C-O} adsorption of derived carboxylic acid groups, respectively, referred to small molecular carboxylic acids [30,31]. In contrast, a more broad absorbance around 3000 cm^{-1} also indicates the existence of hydrogen-bonded-COOH groups on the backbone of SMA (refer to the later discussions).

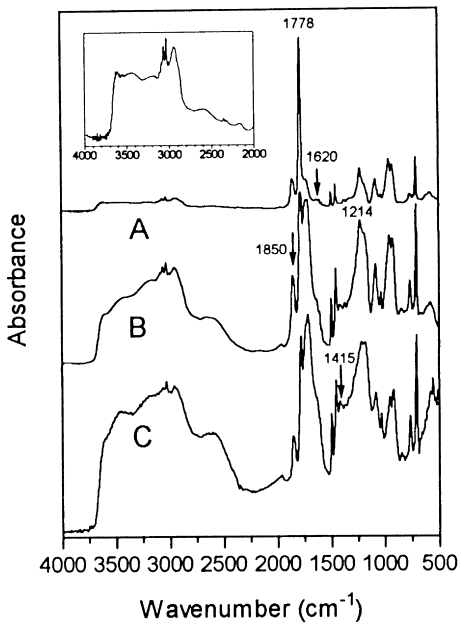

Fig. 5. FT-IR spectra for samples in Fig. 2: (a) SMA–H_2O–2; (b) SMA–H_2O–6, (c) SMA–H_2O–HCl. The IR spectrum of A in the region of 4000–2000 cm^{-1} is magnified (ca. 7 ×) in absorbance to show the information on the band at 2600 cm^{-1} and carbon dioxide probably absorbed in the sample (inset).

The band at 1710 cm^{-1} for SMA–H_2O–2 sample(Fig. 5a) is much weaker than that for SMA–H_2O–6 (Fig. 5b) and SMA–H_2O–HCl (Fig. 5c) with the band at 700 cm^{-1} as an internal reference. It is evident that SMA in SMA–H_2O–2 system hydrolyzed only to a small degree within the reaction time (i.e., 2 h), while in the SMA–H_2O–HCl system or in SMA–H_2O–6 within a longer reaction time (ca. 6 h) more maleic acid groups on the backbone chains were produced by the hydrolysis of SMA.

Fig. 2c shows that holes in the thin film were not formed even though there were carboxylic acid groups on the backbone of SMA in SMA–H_2O–6 system. The surface pattern of the film in such a case could be regarded as being controlled by surface energy effect and water domains, as in the case of Fig. 2b for SMA–H_2O–2 sample. It is assumed that the formation of well-arrayed and uniform-sized hole pattern on the surface of hydrolyzed SMA copolymer results from the existence of both carboxylic acid groups on the backbone chains and HCl in the system, wherein HCl is crucial in the formation of holes.

3.3.2. Hydrogen bonding between carboxylic acid groups on the backbone chains

It has been well known that in the liquid or solid state, and in not a very dilute solution in non-polar solvents, carboxylic acids often exist as dimers because of strong hydrogen bonding. Carboxylic acid dimers display very broad, intense O–H stretching absorption in the region of 3300–2500 cm^{-1}, which differs from the strong absorption of a free hydroxyl stretching vibration (near 3560–3500 cm^{-1}) [31,32]. The band usually centers near 3000 cm^{-1}. The IR absorption profiles between 3700 and 2310 cm^{-1} in Fig. 5 with C–H stretch around 2950 cm^{-1} superimposed upon O–H stretch indicate that sample SMA–H_2O–6 and SMA–H_2O–HCl display strong hydrogen bonding between two carboxylic acid groups. It can be seen that the O–H stretching absorption region in Fig. 5 is wider than that for the usual carboxylic acid dimers (i.e. 3300–2500 cm^{-1}). Perhaps, this widening of ν_{O-H} should be attributed to the influence of carbon dioxide and water absorbed in the sample during measurements, because carbon dioxide [31] has absorption bands at 3700–3500 and 2380–2220 cm^{-1} regions and water [30] has absorption around 3500 cm^{-1}, and the existence of absorbed water in these three samples can also be indicated by the band at 1620 cm^{-1}. Known from the inset of Fig. 5, sample SMA–H_2O–2 also displays absorption of carbon dioxide, and is only suppressed by the absorption of the maleic anhydride groups on the backbone chains. Of course, the existence of copolymer chains in our case will also inevitably make the stretching absorption of O–H of –COOH a little different from that of small molecular carboxylic acids.

Apart from the interference of carbon dioxide and water, the broad O–H stretching absorption profiles of SMA–H_2O–6 and SMA–H_2O–HCl samples, especially the existence of the band at 2600cm^{-1}, are consistent with the small molecular carboxylic acid dimers caused by the hydrogen bonding, such as heptanoic acid [31], and acetic acid and 2-butenoic acid [30], it is reasonable that the absorption band at 2600 cm^{-1} is the result of hydrogen bonding in carboxylic acids. Hence, the IR absorption band at 2600 cm^{-1} for samples SMA–H_2O–6 and SMA–H_2O–HCl is the O–H stretching vibration caused by the strong hydrogen bonding between carboxylic acids groups. There is almost no absorption at 2600 cm^{-1} in SMA–H_2O–2 or SMA (Fig. 1a) compared with SMA–H_2O–6 and SMA–H_2O–HCl, namely, there are very few or no hydrogen bonding effects in them, this is because there are almost no carboxylic acid groups in the former two samples. It should be noted that the hydrogen bonding will form between carboxylic acids both on intramolecular and intermolecular chains.

3.3.3. Formation of holes

It is known that copolymers of maleic acid with low molecular weight can act as anionic polymer surfactants [54,55], carboxylic acid groups on the backbone are hydrophilic and can enter the water phase. As surfactants, these polymers should not entirely dissolve in water, but the solubility of these anionic surfactants change with the pH of the solution. Low pH value reduces the dissociation of –COOH groups and the solubility of the surfactant in the water is reduced [54]. In contrast, the state of hydrogen bonding of –COOH groups should be taken into account. The formation of these hydrogen bonds between carboxylic acid groups will exist in the THF solutions, and change the

chain conformation. It can be easily understood that such hydrogen bonds, undoubtedly, make the backbone chains more coiled or even "crosslinked" with O=COH…O=C(OH) groups, this state will undoubtedly affect the interaction (hydrogen bonding) between water and –COOH groups.

However, in the acidified THF solutions, more H^+ cations in the solution will easily protonate –COOH to form $-COOH_2^+$ groups on the backbone of the copolymer as viewed from chemistry, though there are no direct experimental evidences on the protonation of COOH groups in our SMA system. Electrostatic repulsion between these cations may reverse the approach of carboxylic acid groups to form hydrogen bonds, and make the backbone chains more extended, leading to a suspension of $-COOH_2^+$ in an "isolated" state on the backbone chains. These effects of HCl would be favorable for the emulsifying effect of hydrolyzed SMA, because in such cases the –COOH or $-COOH_2^+$ groups are not buried in the coiled chain aggregates, and enter the water phase easily.

Moreover, Fig. 5 shows that carboxylic acid groups in SMA–H_2O–HCl sample undoubtedly form strong hydrogen bonds, which contradicts the protonation suggested for COOH groups. The IR samples were dried before IR measurements, and HCl was eliminated from the samples during drying, namely, a reverse reaction of protonation occurred. Hence, the sample SMA–H_2O–HCl shows a similar absorption behavior to that of SMA–H_2O–6 within 3300–2500 cm^{-1}.

In as-described THF solutions of SMA copolymer, COOH groups on the backbone chains can also form hydrogen bonds intermolecularly with water and THF that acts as proton acceptor [31]. These hydrogen bonds will not make the backbone chains coiled, for these small molecular moieties only suspend on the polymer chains.

The formation of well-arrayed and uniform-sized holes in SMA–H_2O–HCl system can be explained by the surfactant effect of hydrolyzed SMA. Hydrolyzed SMA dissolves slightly in water, and hardly in acidified water [20]. In our opinion, the formation of holes are mainly the traces of water droplets emulsified by hydrolyzed SMA during the evaporation in casting, and the surface energy in this case is not controlling. It is a fact that a mixed solvent, consisting of THF and water, was used in preparing sample solutions for the SMA–H_2O–HCl and SMA–H_2O films, even though the water quantity could be ignored with regard to that of THF. Compared with water, THF is of a much lower boiling point (i.e. 66°C/1 atm.) and higher volatility, so the volatilization process in spin-casting can be divided into two stages, THF and water volatilization.

During the first stage, THF volatilized, and water phase separated from the polymer; at the same time, the pH value of the system decreased with the evaporation of solvent resulting in a higher degree of protonation of –COOH groups. Then, water phase surrounded by the polymer volatilized when the first stage was completed, and the whole volatilization proceeded into the second one. The water phase was surrounded by the hydrolyzed SMA molecules in SMA–H_2O–HCl cases. The surfactant effect of hydrolyzed SMA led to stable, well-arrayed and uniform-sized water droplets containing chlorine (Cl^-) as counterions on their surfaces when the second stage took place, and the hole structure formed in the film when these water droplets volatilized.

It can be shown in Figs. 2b and 2c that SMA–H_2O–2 and SMA–H_2O–6 films take a surface pattern similar to SMA, a bicontinuous pattern. It indicates that there were no regular, droplet-like, water domains in these cases, the poor surfactant effect of SMA and hydrolyzed SMA in this case should be responsible for this surface pattern. The reasons for these poor surfactant effects can be explained as follows: there are few hydrophilic carboxylic acid groups on the backbone in SMA–H_2O–2 samples, while in SMA–H_2O–6 system the backbone chains may be more coiled, more carboxylic acid groups are hydrogen bonded and buried in the aggregates of coiled chains resulting in a poor hydrophilic property needed by a surfactant in this case.

In experiments, we did not obtain the images with polymer as a dispersed phase which would results in mounds or isolated protrusions on the substrate when the water content was proportionately largest by weight in our tested composition ranges. This phenomenon indicates that there were both mobile (mixed and evaporate with THF together) and bound (interacting with polymer, e.g. via hydrogen bonds) water populations in the solutions, and an equilibrium water concentration bound to the copolymers, as in the case of bound solvent population by the polymer in spin-cast thin film of poly(3-methyl-4-hydroxy styrene) (PMHS) with propylene glycol methyl ether acetate (PGMEA) as solvent [9]. The bound water volatilizes in the second stage during casting, and is the origin for the hole and valley pattern in the films of SMA–H_2O–HCl and SMA–H_2O–2(-6) samples, respectively. The difference in these two cases may be in that the bound water was further emulsified to form droplets as discussed earlier in the former case, but not in the latter.

Comparing Fig. 2d with Fig. 4c, it can be found that the diameter of the holes mainly depends on the concentration of the cast solution, i.e. on the thickness of the films. The same phenomenon was also observed in dPS/PVME blends, as mentioned by Ermi et al. in their recent article [14], their results showed that the hole diameter scales roughly in proportion to the film thickness.

The interactions between the film matrix and substrates can influence, but not always, the surface pattern of thin polymer blend films, reflected by the dewetting properties of the polymer matrices on the substrates, as shown by other authors [12]. But, we did not take interactions between the film matrix and silicon wafer into consideration in this discussion. In our opinion, the interactions between film matrix and substrate should not be the dominantly affecting factors in controlling the surface patterns of our films, not

the origin of the hole formation. SMA–H_2O–2 (or SMA) and SMA–H_2O–6 showed a similar surface pattern, however, their compositions differed a lot as identified by IR spectra, i.e. the interactions in these samples were different. In addition, these surface patterns in Fig. 2, especially the hole structure can be observed in other substrates, such as quartz and glass slide.

4. Conclusion

Maleic anhydride moieties on the backbone chains of SMA hydrolyze in a THF solution containing water, and hydrochloric acid accelerates the hydrolysis. Distinct surface patterns in the thin films of poly(styrene–maleic anhydride) alternating copolymer (SMA) spin-cast from different THF solutions were observed with AFM. Well-arrayed and uniform-sized holes were formed in the thin films when hydrochloric acid was added to the solution mixture. HCl can also influence the hydrogen bonding between carboxylic acid groups in THF solution, and is crucial for the formation of hole pattern. The formation of the holes is interpreted as the trace of water droplets which are emulsified by the hydrolyzed SMA during casting. In the solution mixture, both mobile and bound water populations would be present and the traces of bound water are responsible for the hole pattern of as-cast thin films. It still remains to be investigated how the degree of hydrolysis of SMA influence the surface pattern of the thin film, and factors influence the film thickness and hole size.

Acknowledgements

We appreciate the National Nature Science Foundation of China for supporting this work. We are grateful to Dr. Zheng Jiao (Hefei Institute of Intelligent Machine, Academia Sinica) for ellipsometric measurements of the thin SMA films, and referees involved in revision for their generous advice.

Appendix A

The calculation formula for mole fraction, χ, of styrene in the copolymer was derived as following: Given A, B represents the protons in $-CH_2-$ and $-CH-$ of styrene, respectively, and C for the protons of maleic anhydride. Use I to represent the ^1H NMR integration intensity, and a subscript indicates the kinds of protons, e.g., $I_{(\text{phenyl})}$ and $I_{(\text{Total})}$ represent the integration intensity of phenyl protons and total protons, respectively. Hence,

$$\chi = \frac{I_{(\text{phenyl})}/5}{I_{(\text{phenyl})}/5 + I_{(\text{C})}/2}$$

for $I_{(\text{C})} = I_{(\text{Total})} - I_{(\text{A})} - I_{(\text{B})} - I_{(\text{phenyl})}$, and $I_{(\text{A})}/2 = I_{(\text{phenyl})}/5 = I_{(\text{B})}$, then formula (Eq. (1)) in the text will be obtained.

References

[1] Odian G. Principles of polymerization. 2. New York: Wiley, 1981.
[2] Tvivedi BC. Maleic anhydride. New York: Plenum Press, 1982.
[3] Cao K, et al. Polym Bull (in China) 1994;2:97.
[4] Tredgold H. Thin Solid Films 1987;152:223.
[5] Davis F, Hodge P, Towns CR, Ali-Adib Z. Macromolecules 1991;24:5695.
[6] Zhou W, Dong J, Qiu K, Wei Y. Acta Polymerica Sinica 1998;3:345.
[7] Zhao Z, Gao Z, Ou Y, Qi Z, Wang F. Acta Polymerica Sinica 1996;2:228.
[8] Huang Z, Qiu K, Wei Y. J Polym Sci: Part A: Polym Chem 1997;35:2403.
[9] Frank CW, Rao V, Despotopoulou MM, Pease RFW, et al. Science 1996;273:912.
[10] Thompson LF, Grant WC, Bowden MJ. Introduction to lithography. 2. Washington, DC: American Chemical Society, 1994. p. 308.
[11] Bornside DE, Macosko CW, Scriven LE. J Imag Tech 1987;13:123.
[12] Dalnoki-Veress K, Forrest JA, Stevens JR, Dutcher JR. J Polym Sci: Part B: Polym Phys 1996;34:3017.
[13] Affrossman S, Henn G, O'Neill SA, Pethrick RA, Stamm M. Macromolecules 1996;29:5010.
[14] Ermi BD, Karim A, Douglas JF. J Polym Sci: Part B: Polym Phys 1998;36:191.
[15] Karim A, Slawecki TM, Kumar SK, Douglas JF, et al. Macromolecules 1998;31:857.
[16] Tanaka K, Takahara A, Kajiyama T. Macromolecules 1998;31:863.
[17] Meiners JC, Elbs H, Ritzi A, Mlynek J, Krausch G. J Appl Phys 1996;80(4):2224.
[18] Masuda H, Fukuda K. Science 1995;268:1466.
[19] Masuda H, Satoh M. Jpn J Appl Phys 1996;35(1):L126.
[20] Braun D, Cherdron H, Kern W. Techniques of polymer synthesis and characterization. New York: Wiley, 1972.
[21] Reiter G. Langmuir 1993;9:1344.
[22] Ebdon JR, Towns CR, Dodgson K. J Macromol Sci Rev 1986;C26(4):523.
[23] Deb PC, Meyerhoff G. Eur Polym J 1984;20(7):713.
[24] Tsuchida E, Tomono T, Sano H. Makromol Chem 1972;151:245.
[25] Liu C, Zhao Y, Guo L. Experiments for polymer chemistry. China: Press of University of Science and Technology of China, 1988.
[26] Hill DJT, O'Donnell JH, O'Sullivan PW. Macromolecules 1985;18:9.
[27] Dérand H, Wesslén B. J Polym Sci: Part A: Polym Chem 1995;33:571.
[28] Prouchert CJ. The Aldrich Library of Infrared Spectra, 3rd ed. Aldrich Chemical Company, Inc., No. 20,061-1, 1981.
[29] Yoshinaga K, Sueishi K, Karakawa H. Polym Adv Tech 1996;7(1):53.
[30] Shi Y, Sun X, Jiang Y, Zhao T, Zhu H. The spectroscopy and chemical identification of organic compounds. Jiangsu Press of Science and Technology, 1988.
[31] Silverstein RM, Bassler GC, Morrill TC. Spectrometric identification of organic compounds. 5. New York: Wiley, 1991.
[32] Dyke SF, Floyd AJ, Sainsbury M, Theobald RS. Organic spectroscopy: an introduction. 2. New York: Longman, 1978.
[33] Bark LS, Allen NS. Analysis of polymer system. London: Applied Science Publishers, 1982.
[34] Shashidhar GVS, Ranga Rao K, Satyanarayana N, Sundaram EV. J Polym Sci: Part C: Polym Lett 1990;28:157.
[35] Barron PR, Hill DJT, O'Donnell JH, O'Sullivan PW. Macromolecules 1984;17:1967.
[36] Magonov SN, Reneker DH. Annu Rev Mater Sci 1997;27:175.
[37] Chen JT, Thomas EL. J Mater Sci 1996;31:2531.
[38] Reiter G. Phys Rev Lett 1992;68(1):75.
[39] Mayes AM. Macromolecules 1994;27:3114.
[40] Kajiyama T, Tanaka K, Takahara A. Macromolecules 1995;28:3482.
[41] Tanaka K, Takahara A, Kajiyama T. Acta Polym 1995;46:476.
[42] Tanaka K, Taura A, Ge S-R, Takahara A, Kajiyama T. Macromolecules 1996;29:3040.
[43] Kajiyama T, Tanaka K, Takahara A. Macromolecules 1997;30:280.

[44] Affrossman S, Hartshorne M, Jerome R, Pethrick RA, Petitjean S, Vilar MR. Macromolecules 1993;26:6251.
[45] Affrossman S, Bertrand P, Hartshorne M, Kiff T, Leonard D, Pethrick RA, Richards RW. Macromolecules 1996;29:5432.
[46] Sugiyama A, Hirao A, Nakahama S. Macromol Chem Phys 1996;197:3149.
[47] Jalbert CJ, Koberstein JT, Balaji R, Bhatia Q, et al. Macromolecules 1994;27:2409.
[48] Koberstein JT. MRS Bull 1996;21:19.
[49] Shirota Y, Yoshimura M, Matsumoto A, Mikawa H. Macromolecules 1974;7:4.
[50] Rätzsch M, Arnold M, Hoyer R. Plaste Kautsch. 1977;24:731.
[51] Fukuda T, Ma Y-D, Inagaki H. Macromolecules 1985;18:17.
[52] Sato T, Abe M, Otsu T. Makromol Chem 1977;178:1061.
[53] Faldi A, Composto RJ, Winey KI. Langmuir 1995;11:4855.
[54] Liu C, Jiang X, Li B, Zhang W. Encyclopedia of surfactant application. China: Press of Beijing University of Technology, 1992. p. 47.
[55] Mark HF, Gaylord NG, Kales NMB, editors. Encyclopedia of polymer science and technology, 1. New York: Interscience Publishers (a division of Wiley), 1964. p. 81–84.